Available online at www.sciencedirect.com
SCIENCE DIRECT®
Proceedings of the Combustion Institute 30 (2005) 1343–1351
Proceedings of the Combustion Institute
www.elsevier.com/locate/proci

The relative roles of acetylene and aromatic precursors during soot particle inception

Angela Violi[a,*], Gregory A. Voth[b], Adel F. Sarofim[a]

[a] Department of Chemical Engineering, University of Utah, Salt Sake City, UT 84112, USA
[b] Henry Eyring Center for Theoretical Chemistry, Department of Chemistry, University of Utah, Salt Sake City, UT 84112, USA

Abstract

Kinetic Monte Carlo (KMC) and Molecular Dynamic (MD) methodologies were applied sequentially to simulate soot inception in premixed fuel-rich benzene flames to identify the role of accessibility to reaction sites on the relative rate of reactions of molecules of different size. This approach is designed to provide atomistic scale structure (bonds, bond-angles, and dihedral angles) as soot precursors evolve into a three-dimensional structure. Two different times in a benzene flame, experimentally studied by Homann were chosen to examine the reaction sequence between 20 gas phase species and the soot seed, starting with pyrene. The curvature of the seed particle is found to increase with particle size becoming significant when the number of carbon atoms exceed 100 and with the seed developing a spheroidal shape when the number of carbon atoms exceeds 400. The curvature increases with temperature in the flame, being greater at 2100 than at 1700 K. The accessibility of the sites on the growing seed molecule decreases with increases in curvature of the seed particle and size of the reacting molecule. The accessibility decreases from 1 at a seed size of around 100–150 carbons atoms down to about 0.5 at a size of 400 carbon atoms for acetylene and down to about 0.3 at a seed size of 200 atoms for acenaphthylene. These results show the value of the KMC/MD methodology, which provides insights into the details of soot particle inception.
© 2004 The Combustion Institute. Published by Elsevier Inc. All rights reserved.

Keywords: Nano-particles; Kinetic Monte Carlo; Molecular dynamics

1. Introduction

The processes involved in soot precursor formation exhibit a wide range of time scales, spanning pico- or nanoseconds for intramolecular processes to milliseconds for the formation of the first soot precursors. To accurately describe the soot formation process, it is important to model reactions occurring at different time scales, and at the same time to characterize the product particles in terms of chemical structure/components. Structure–pathways and structure–property relationships may lead to a deeper understanding of soot growth mechanisms. We address these questions theoretically by studying the growth of molecules in combustion environments, using Kinetic Monte Carlo (KMC) and Molecular Dynamics (MD) methodologies.

This approach allows us to follow the growth of aromatic compounds up to the nano-size range in a chemically specific way. It is designed to preserve atomistic scale structure, as bonds, bond-angles, and dihedral angles. Some preliminary

* Corresponding author. Fax: +1 801 585 1456.
E-mail address: violi@eng.utah.edu (A. Violi).

1540-7489/$ - see front matter © 2004 The Combustion Institute. Published by Elsevier Inc. All rights reserved.
doi:10.1016/j.proci.2004.08.226

results have been reported in earlier publications on the evolution of soot precursors in premixed laminar flames [1–4].

In the following sections, the methodology employed in this study is summarized, and then applied to the molecular growth process in a low pressure benzene flame.

2. Methodology

The simulation methods for many-body systems can be divided into two classes of stochastic and deterministic simulations, which are largely covered by Monte Carlo method and MD method, respectively. KM simulations solve the evolution of an ensemble of particles in configuration space, provided some initial condition, and a complete set of transition events (chemical reactions, diffusion events, etc.). By contrast MD solves the trajectories of a collection of atoms in phase space (configuration + momentum) given the initial conditions and potential. This is an advantage of MD simulation with respect to KMC since not only is the configuration space probed, but also the whole phase space, which can give more information about the dynamics of the system, subject to any additional constraints on the equations of motion. However, the limitation in the accessible simulation time represents a substantial obstacle in making useful predictions with MD. Resolving individual atomic vibrations requires a time step of approximately femtoseconds in the integration of the equations of motion, so that reaching times of microseconds is very difficult. The two methods, therefore, differ in their effective ability to explore conformation space. On the other hand, the combination of the KMC and MD methods allows us to span a much wider range of time-scales, while retaining full atomistic detail. This synthesis of methods allows high energy barrier reactions to be effectively included in the nanoparticle growth dynamics. The capability to generate such states directly has many advantages, including bypassing configurations which may be difficult to escape dynamically with MD alone, i.e., MD may not be able to cross the barriers between the conformations sufficiently often to ensure that each conformation is sampled according to the correct statistical weight. MD, on the other hand, can be very useful for exploration and equilibration of the local configurations, whereas the KMC method is more effective in treating transitions and reactions which jump to completely different regions of conformation space via high energy barriers. The latter processes become exponentially slow in the MD algorithm.

During the KMC module [5–7], one reaction from a list of possible events is chosen randomly weighted by the rate constant, and the reaction is allowed to proceed. The clock is then incremented in a way that is consistent with the rate constants for the possible reaction selected. The time-step for a single KMC iteration is a "real time," determined by the kinetics system. The reaction rates among the compounds present in the system are specified as probabilities, and the surface configuration over time is then given by a master equation, describing the time evolution of the probability distribution of system configurations.

MD allows for relaxation of the molecules towards thermal equilibrium. Within the MD module, the potential used to describe hydrocarbon interactions is the adaptive intermolecular reactive bond order (AIREBO) [8] and it is based on the reactive empirical bond-order potential of Brenner [9–11]. The potential describes the covalent bonding interactions largely as in Brenner's REBO potential [12]. In addition, there are terms in the energy to account for torsional energies of single-bond rotations, as well as the non-bonded van der Waals interactions. The torsional energy is modeled as a pairwise interaction between atoms. The advantage of this formulation lies in the fact that the symmetry of the dihedral angle potential is dictated by the symmetry of the molecule, and can change as reactions occur. The van der Waals interaction is modeled using the Lennard-Jones 12-6 potential. The thermodynamic ensemble realized for the MD module is the canonical one (N, V, T), where, the number of particles, the volume, and the temperature are fixed to prescribed values. Of the different methods available for setting the temperature to an assigned value during a simulation, the integral thermostat is selected to dampen temperature fluctuations. It introduces additional degrees of freedom into the system's Hamiltonian for which equations of motion can be derived. The method developed by Nosè [13] uses an external heat reservoir to keep the temperature of the system constant, adding one additional degree of freedom. The thermal interactions between a heat reservoir and the system result in a change of the kinetic energy, i.e., the velocity of the particles in the systems. In this study, we used the Nosè–Hoover thermostat [14,15].

Figure 1 shows a schematic representation of the KMC/MD code. Since the output of the KMC module is a configuration space, while the input to the MD part is represented by the phase space (configuration + momentum), velocities are assigned to the atoms of the growing seed according to a Maxwell–Boltzmann distribution function before entering the MD module.

2.1. Conditions

The environment within which particles are grown is that of a low-pressure benzene–oxygen flame C/O = 0.8 with an unburned velocity of

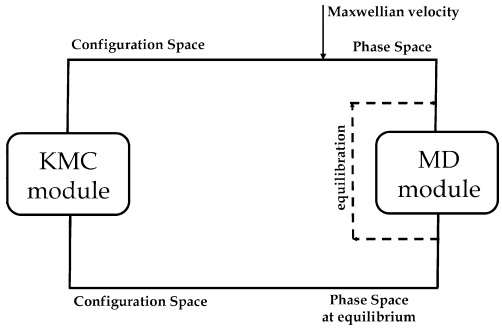


Fig. 1. Schematic representation of the KMC/MD code.

42 cm s^{-1}, $p = 2.66$ kPa. This flame has been experimentally studied by Keller et al. [16], who measured PAH, PAH radicals, and PAH ions by means of resonant (REMPI). Two positions in the flame were selected, corresponding to temperatures of 1700 K at 8 mm and 2100 K at 10 mm. The simulations are started with a seed of pyrene. The current KMC/MD code allows for the reactions with the seed of H, H_2, CH_4, CH_3, C_2H_2, C_2H, C_2H_3, C_2H_5, C_3H_3, C_5H_5, C_5H_6, acenaphthylene, and all its radicals, naphthalene, and all its radicals, biphenyl, phenylacetylene, and styrene. Also included in the list of the possible reactions are cyclodehydrogenation reactions that can occur on the growing seed. These reactions involve the loss of hydrogen atoms to form a new ring. For these types of reactions, the sites identified by the code are for five- and six-member rings: HCCCCC*/HCCCCCC* chains prone to form a new ring by H elimination, and HCCCCCH/HCCCCCCH chains prone to form a ring through elimination of H_2. More details regarding the sites definitions are reported elsewhere [1]. In a situation such as the one defined by the first set of sites, the code removes the terminal H from the chain and then closes the ring. With the second set of sites, the KMC/MD code removes the two terminal hydrogens and forms a new ring. Microscopic reversibility and fragmentation reactions are also included in the newer version of the KMC/MD code. Fragmentation reactions are reactions where a radical breaks apart to form either a stable species and a new radical or two radicals [2,17].

The concentration profiles of the gas-phase species that can contribute to the molecular growth of the aromatic compound have been calculated using the CHEMKIN package [18] together with a kinetic model previously developed by Richter et al. [19]. The resulting temperature and concentration profiles are supplied to the KMC/MD code. In using these concentrations in the atomistic model, no allowance was made in the calculated hydrocarbons and H profiles for species depletion or temperature change. The concentrations of the reactants of interest for the current simulations at the two flame locations are reported in Table 1.

Table 1
Gas-phase species concentrations included in the KMC/MD code at two distances in the flame

Flame height	7 (mm)	10 (mm)
Temperature (K)	1800	2130
H	1.33E−3	6.74E−3
H_2	1.11E−1	1.25E−1
CH_4	2.81E−3	2.49E−3
CH_3	1.30E−3	2.66E−3
C_2H_2	3.62E−2	5.52E−2
C_2H	3.00E−6	3.45E−3
C_2H_3	8.60E−5	1.74E−4
C_2H_5	4.00E−8	1.40E−8
C_3H_3	2.8E−3	3.68E−3
C_6H_6	6.56E−2	2.14E−4
C_6H_5	1.64E−4	3.53E−7
Indene	4.03E−5	8.51E−7
Indenyl	4.70E−5	4.32E−5
$C_{10}H_8$–naphthalene	4.01E−4	4.83E−5
$1^*C_{10}H_7$	1.02E−6	5.94E−9
$2^*C_{10}H_7$	2.03E−6	4.72E−6
$C_{12}H_8$ (acenaphthylene)	1.75E−4	9.91E−5
$1^*C_{12}H_7$	5.70E−7	2.23E−6
$3^*C_{12}H_7$	2.76E−6	1.11E−5
$4^*C_{12}H_7$	2.27E−6	7.31E−6
$5^*C_{12}H_7$	2.20E−6	6.40E−6
Biphenyl	7.32E−6	3.09E−8
C_5H_5	4.15E−3	7.72E−5
$A1C_2H$ (phenyl–acetylene)	7.00E−6	1.32E−5
Styrene–C_8H_8	3.90E−5	2.09E−7

3. Results

Within the KMC/MD code, we evolve time using the KMC simulation module. New molecules are introduced on the surface of the growing seed with a specific kinetic energy and angle. When this happens, we set up an MD simulation to equilibrate the new structure and correctly describe the configuration. We then feed the result back into the KMC module, and continue.

Figure 1 shows a schematic representation of the KMC/MD code. Since the output of the KMC module is a configuration space, while the input to the MD part is represented by the phase space (configuration + momentum), velocities are assigned to the atoms of the growing seed according to a Maxwell–Boltzmann distribution function before entering the MD module.

As shown in Fig. 1, the code alternates between KMC and MD steps during the simulation: as first step of the iteration, the KMC/MD reads the gas-phase concentrations, and then it identifies every atom on the growing seed with a local environment which fits the definition of each site given as input to the code. After checking, if there is enough room next to the site for a gas-phase specie

to penetrate and react, it computes the kinetic rate constants and the reaction rates for the possible reactions, and then it selects a reaction with probability proportional to its rate. After randomly selecting a site for the reaction chosen, the KMC module modifies the site according to the reaction transition. At this point, the MD module is used to perform energy minimization. The molecule is now ready for the next iteration in which the reaction sites of the new updated particle are counted. This atomistic approach allows us to follow the growth of particles in a chemical specific way, and Fig. 2 shows some results obtained with the KMC/MD code. The H/C ratio, the mass, and the aspect ratio of *f* the growing seed are reported as a function of time.

The aspect ratio has been computed as the ratio of the axes of the ellipse that has as its center the object's centroid [2]. With this approach it is possible, as can be seen from Fig. 2, to reach a time scale of the order of milliseconds.

A different procedure is applied during the MD run for ring closure reactions that increase the extension of aromatic islands inside the structure, as illustrated in Fig. 3. Snapshots of the configuration changes (in terms of bond lengths and dihedral angles for carbons 1–5) during a cyclodehydrogenation reaction are shown.

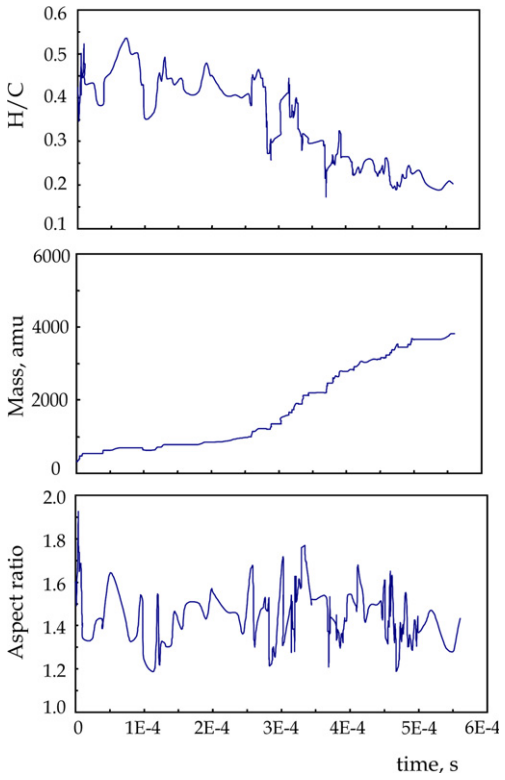


Fig. 2. KMC/MD calculations of H/C ratio, mass, and aspect ratio of a growing seed as function of time.

The starting structure (Structure 1) is produced by the KMC simulation: an acetylene molecule is added to the radical on C5 of the six-membered ring. For the first 2 ps, after the H_2 elimination, the C1–C2 distance between the ends of the chain of the six-membered rings are gradually brought together, while all other atoms are allowed to relax. We have obtained reliable results by using increments of 5E−6 Å for closing the rings [3]. After the ring has been closed, full relaxation is performed for a few ps that allows the structure to reach a relaxed local minimum. Changes in bond lengths and angles are shown in Fig. 3. Figure 4 reports the energy of the system versus the MD time during for the cyclodehydrogenation reaction shown in Fig. 3. The first 2 ps are for the constrained dynamics, followed by 4 ps for the system to equilibrate. At this point, the molecule is ready for the next iteration in which the reaction sites of the new updated particle are counted, and a new reaction is chosen by the KMC module.

3.1. Accessibility

The rate for a typical gas-surface reaction is $r = kC_gN_s$, where k is the pressure and temperature dependent rate constant, C_g is the gas-phase concentration, while N_s is the surface-site density or number for a particular reaction in which gas-species g reacts with a particular surface-site s. The real structure of a compound is decomposed into one that is defined by an array of surface positions. To have a sense of the time associated with the KMC module, Table 2 reports the sequence of reactions performed by the code during one trajectory together with the corresponding KMC time. To choose one of the reactions, a list is constructed which contains a running sum of the rates at each of the possible events, and each entry of the list is normalized by the sum of the rates of all possible events. Once the list is constructed, a random number in the range $(0, 1)$ is chosen and compared with the list of summed relative rates, and one of the events is chosen. We use a variable time increment that allows us to consider reactions that occur on widely disparate time scales. If fast reactions are involved, the denominator is small, and the time scale is fine. When only slow reactions are possible, the time scale is coarse.

One of the characteristics of the growth process is represented by the accessibility of the gas-phase species to the reactive sites on the seed. During the site-counting procedure, the code identifies every atom with a local environment that fits the definition of each site listed as input to the KMC/MD code. At the same time, it also checks if there is sufficient space next to the site for a gas-phase species to penetrate and react. In this way, an atom is considered as a possible site for termination or addition by a gas-phase species only if

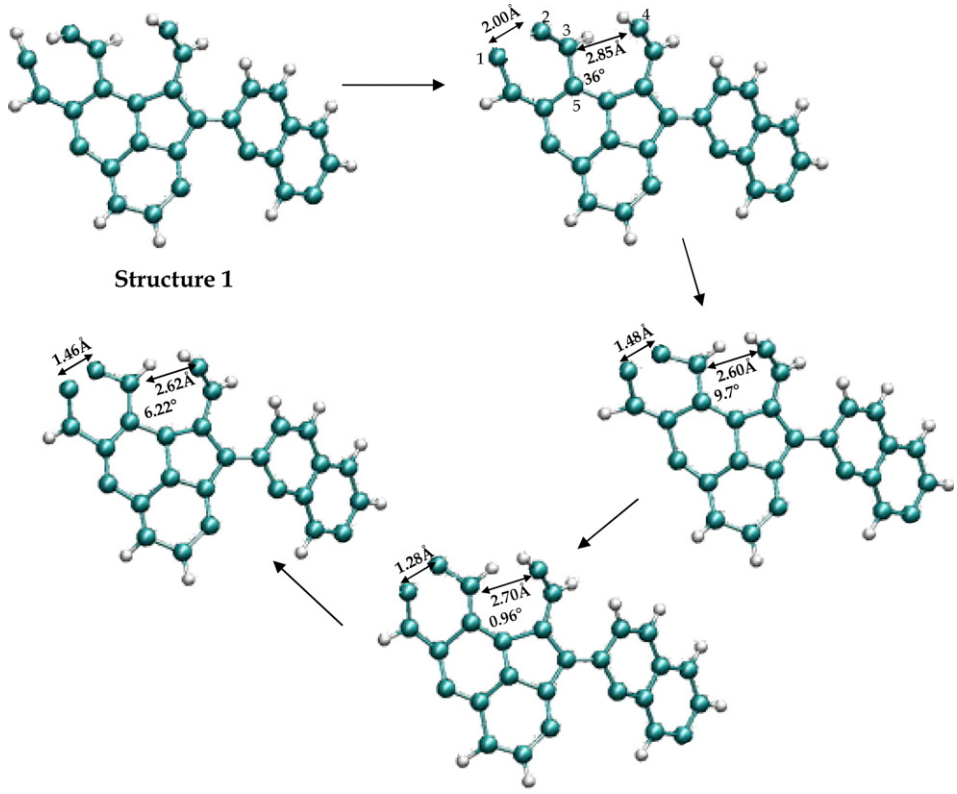


Fig. 3. Snapshots of configuration changes (in terms of bond lengths and dihedral angles for carbons 1–5) during a cyclodehydrogenation reaction.

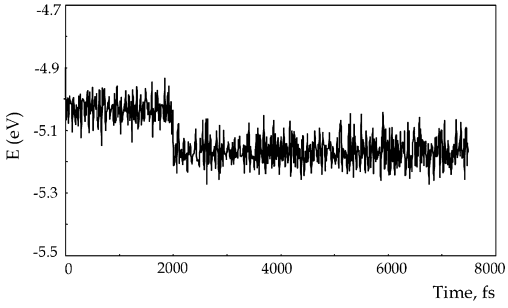


Fig. 4. System energy versus MD time for the cyclodehydrogenation reaction shown in Fig. 3.

the gas-phase species of interest can be accommodated. The code goes over all atoms in the cluster, including all the possible sites, even the "hidden" ones that may be located inside the structure. Once the site is found, the code loops over species that may be added to that specific site. The spherical volume around each adduct atom is computed, and if the space around the site is large enough for a specific species to fit in, then the site is accepted, otherwise it is rejected.

As we previously reported, structures formed in aromatic flames show a high degree of curvature, and hence represent interesting structures for which the steric effects are significant [19]. The capability of the KMC/MD code to study the accessibility of gas-phase species in the low pressure benzene flame studied by Keller et al. [16] is reported for two different distances from the burner, the first within the oxidation zone (8 mm), and the second at the flame front (10 mm) (see Table 2).

For a benzene flame, with a C/O ratio of 0.8, the benzene concentration exceeds that of acetylene up to a height of about 8 mm ($T \approx 1800$ K). Higher in the flame, acetylene concentrations will exceed those of benzene. As a consequence, the relative contributions to the growth of soot precursors, hence particle morphology, will change as combustion progresses, with benzene dominating early in the flame and acetylene and its derivatives dominating at later stages of combustion. Starting from pyrene we ran several trajectories to describe the evolution in time of the particles configurations. An ensemble of seeds with different sizes spanning a few C atoms to 400 C atoms was computed in the benzene flame environment

Table 2
List of the reactions picked by the KMC module for 2 ps of simulation

Time (s)	Reactions
2.14E−7	H abstraction from six-membered ring by H atom
2.55E−7	C_6H_6 addition to radical on six-membered ring
2.69E−7	H abstraction from six-membered ring by H atom
5.6E−7	C_6H_6 addition to radical on six-membered ring
6.46E−7	Dehydrogenation reaction to form six-membered ring—site HCCCCCCH
7.64E−7	H addition to radical on six-membered ring
7.91E−7	H abstraction from six-membered ring by H atom
8.17E−7	H addition to radical on six-membered ring
8.28E−7	C_2H_2 abstraction from the seed
8.42E−7	H addition to radical on six-membered ring
9.5E−7	H abstraction from six-membered ring by H atom
1.14E−6	Dehydrogenation reaction to form five-membered ring—site HCCCCCH
1.15E−6	C_6H_6 addition to radical on five- membered ring
1.26E−6	H abstraction from six-membered ring by H atom
1.27E−6	H addition to radical on six-membered ring
1.48E−6	H addition to radical on six-membered ring
1.53E−6	H addition to radical on six-membered ring
1.57E−6	H abstraction from six-membered ring by H atom
1.75E−6	C_6H_6 addition to radical on six- membered ring
1.78E−6	H addition to radical on six-membered ring
1.88E−6	H abstraction from six-membered ring by H atom
1.89E−6	H addition to radical on six-membered ring
1.98E−6	Dehydrogenation reaction to form five-membered ring—site HCCCCCC*
2.07E−6	H addition to radical on five-membered ring

at both 1800 and 2130 K. There is a competition between bimolecular association reactions (addition or growth reactions) and rearrangement reactions which exhibit higher activation energies: at the low temperatures at the beginning of the oxidation zone, the molecules grow but rearrangement and degradation reactions do not play a significant role [20]. With increasing temperature, the growth reactions become faster but the rates of rearrangements become increasingly more rapid. Cage closure reactions, the breaking of C–H bonds, and intramolecular rearrangements have large activation energies and are favored at higher temperature [19]. For this reason, the structures formed at 2100 K have a greater curvature than the one formed at 1700 K. Figure 5 reports the fraction of accepted sites f_a (number of accepted over the sum of accepted and rejected sites) for the addition of acetylene, naphthalene, and acenaphthylene to the growing seed as a function of the number of atoms in the growing seed. These three species represent the key compounds for the aromatic growth. Acetylene is the key component for growth by the HACA mechanism [21], and the aromatic compounds are representative of those taking part in polymerization process involving the reaction of six- and five-membered rings. The HACA mechanism implies a repetitive reaction sequence of hydrogen abstraction by H atom from hydrocarbons and addition of acetylene to the radical site formed which propagates molecular growth and cyclization of PAH. Naphthalene and acenaphthylene are part of the polymerization route based on the formation of resonantly stabilized structures of the reacting radicals, which follows the idea that the growth of aromatic compounds beyond 3-ring PAH is modeled by a radical–molecule sequence of reactions involving five-membered ring compounds [22]. Aromatic radicals then add to the conjugated double bond of five-membered PAH, and they grow until termination reactions occur by coupling of two growing radical intermediates and/or H-atom addition to a radical [23]. Note that the data reported in the graphs are the results of different computed trajectories, which accounts for the scatter of the data for some configurations. Running different trajectories with different random number generators leads to diverse reaction pathways.

For a small seed, up to about 150 C atoms, the accepted fraction of sites is fairly stable with a value of about 1, meaning that all the sites identified by the code are accepted in terms of space available for the gas-phase species to be added. The fraction of accepted sites for acetylene is almost always 1, and only starts to decrease for the larger seed sizes, say 300 C atoms. For naphthalene and acenaphthylene, the decrease in accessibility with increases in the size of the seed is more significant due to the bigger dimensions of these aromatic compounds compared with acetylene, and the fraction of accepted sites decreases to a value of around 0.4 at 350 C atoms.

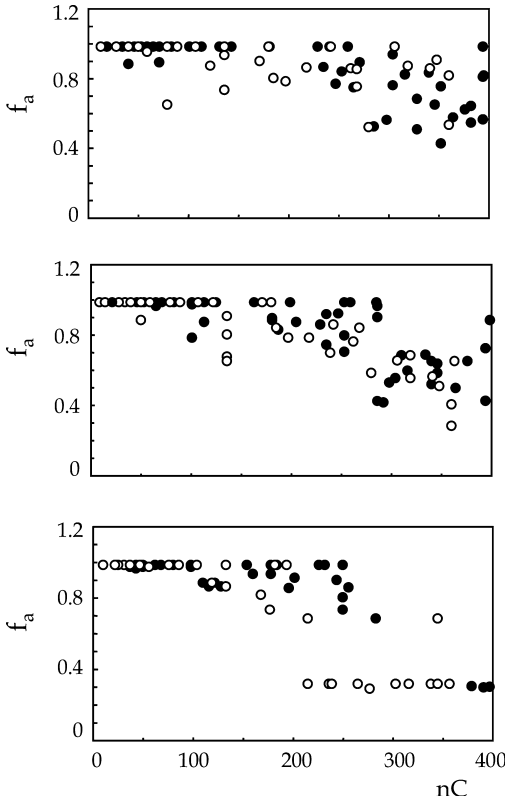


Fig. 5. Fraction of accepted sites (f_a) as function of the number of carbon atoms, for acetylene, naphthalene, and acenaphthylene at 1700 and 2100 K.

For the same number of carbon atoms present in the seed, the fraction of accepted sites is lower at higher temperature, since structures at higher temperatures present a higher degree of curvature compared with those formed at lower temperature.

4. Conclusions

In this paper, a description of the atomistic methodology used to grow nanoparticles at combustion conditions is reported using atomistic methods. kinetic Monte Carlo simulations probe the configuration space by trial moves of particles. By contrast, in the MD simulation the Hamiltonian' equation of motion is integrated to follow the movement and velocities of atoms. The coupling of these two methodologies lead to a powerful tool that can be used to investigate chemical and physical properties of nanoparticles that would not be possible to assess otherwise without the knowledge of their structures. Specifically, we reported detailed computations that show the importance of having MD for processes that occur on the picosecond time scale and kinetic Monte Carlo to boost the time and be able to reach longer times. The accessibility of gas-phase species to the growing seed has been evaluated for some key compounds represented by acetylene, naphthalene, and acenaphthylene. It is shown that the accessibility to reaction sites of the larger aromatic compounds decreases at a faster rate than that of acetylene. This effect is enhanced at the higher temperatures, at which the seed particle shows greater curvature. This shift in relative rates of reactions of aromatic compounds and acetylene is important for explaining the structure of the soot particles, since the aromatic compounds are largely responsible for introducing curvature into soot particles at early times.

Acknowledgments

This research is funded by the University of Utah Center for the Simulation of Accidental Fires and Explosions (C-SAFE), funded by the Department of Energy, Lawrence Livermore National Laboratory, under subcontract B341493 and by a National Science Foundation Nanoscale Interdisciplinary Research Team grant (EEC-0304433). The calculations presented in this paper were carried out at the Utah Center for High Performance Computing, University of Utah that is acknowledged for computer time support.

References

[1] A. Violi, A. Kubota, T.N. Truong, W.J. Pitz, C.K. Westbrook, A.F. Sarofim, *Proc. Combust. Inst.* 29 (2) (2002) 2343–2349.
[2] A. Violi, G.A. Voth, A.F. Sarofim, *Combust. Sci. Tech.* 176 (2004) 991–1005.
[3] A. Violi, A. Kubota, W.J. Pitz, C.K. Westbrook, A.F. Sarofim, *Preprints of Symposia—American Chemical Society, Division of Fuel Chemistry,* vol. 47 (2), 2002, p. 771.
[4] A. Violi, G.A. Voth, A.F. Sarofim, *Preprints of Symposia—American Chemical Society, Division of Fuel Chemistry,* vol. 48 (2), 2003, p. 545.
[5] A.B. Bortz, M.H. Kalos, J.L. Lebowitz, *J. Comput. Phys.* 17 (1975) 10–18.
[6] A.F. Voter, *Phys. Rev. B* 34 (1986) 6819–6829.
[7] K.A. Fichthorn, W.H. Weinberg, *J. Chem. Phys.* 95 (1991) 1090–1096.
[8] S.J. Stuart, A.B. Tutein, J.A. Harrison, *J. Chem. Phys.* 112 (2000) 6472–6486.
[9] D.W. Brenner, *Phys. Rev. B* 42 (1990) 9458–9471.
[10] D.W. Brenner, J.A. Harrison, C.T. White, R.J. Colton, *Thin Solid Films* 206 (1991) 220–223.
[11] D.W. Brenner, *Phys. Rev. B* 46 (1992) 1948–1953.
[12] D.W. Brenner, O.A. Shenderova, J.A. Harrison, S.J. Stuart, B. Ni, S.B. Sinnott, *J. Phys.: Condens. Matter* 14 (2002) 783–802.
[13] S. Nosè, *Mol. Phys.* 52 (1984) 255–261.

[14] S. Nosè, *J. Chem. Phys.* 81 (1984) 511–519.
[15] W.G. Hoover, *Phys. Rev. A* 31 (1985) 1695–1700.
[16] A. Keller, R. Kovacs, K.-H. Homann, *Phys. Chem. Chem. Phys.* 2 (2000) 1667–1675.
[17] A. Violi, G.A. Voth, A.F. Sarofim, *Combust. Flame*, (2004), in press.
[18] R.J. Kee, F.M. Rupley, J.A. Miller, *Chemkin II: A Fortran Chemical Kinetics Package for the analysis of gas phase chemical kinetics*, Report No. SAND 89-8009B, Sandia National Laboratories, 1989.
[19] H. Richter, T.G. Benish, O.A. Mazyar, W.H. Green, J.B. Howard, *Proc. Combust. Inst.* 28 (2000) 2609–2618.
[20] A. Keller, R. Kovacs, K.-H. Homann, *Phys. Chem. Chem. Phys.* 2 (2000) 1667–1675.
[21] M. Frenklach, H. Wang, *Proc. Combust Inst.* 23 (1991) 1559–1564.
[22] A. D'Anna, A. Violi, *Proc. Combust. Inst.* 27 (1998) 425–433.
[23] A. Violi, A.F. Sarofim, T.N. Truong, *Combust. Flame* 126 (1–2) (2001) 1506–1515.

Comments

Katharina Kohse-Höinghaus, University of Bielefeld, Germany. You have modeled the aspect ratio of the particles. What families of reactions is this aspect ratio sensitive to, and is this different for aromatic and aliphatic fuels?

Reply. The aspect ratio decreases with increasing particle size and with increasing aromaticity of the reactants. In the case of aromatic fuels, polymerization reactions can occur early since aromatic compounds are in relatively large concentrations in the fuel, whereas in the case of aliphatic fuels such as acetylene, ethylene, or methane the first aromatic ring must be formed from fuel decomposition products by a sequence of elementary reactions and therefore, the concentrations of aromatic soot precursors are in lower concentrations than in the aromatic flames. For a benzene flame, with a C/O ratio of 0.8, the benzene concentration exceeds that of acetylene up to a height of about 8 mm (T' 1900 K). Higher in the flame, acetylene concentrations will exceed those of benzene. As a consequence, the relative contributions to the growth of the soot precursors will change as combustion progresses, with benzene dominating early in the flame and acetylene and its derivatives dominating at later stages of combustion. The percentage of the carbon growth contributed by benzene decreases from 84% at a flame height of 7 mm to 13.1% at 10 mm. Dehydrogenation reactions, which involve the loss of hydrogen with rearrangement of the structure to form new rings, are 11% of the reactions that occur at 1800 K, and their contributions increase to 22% at 2200 K [1]. The structures formed in aliphatic flame are instead mainly planar and the contribution of acetylene is significant.

Reference

[1] A. Violi, Combust. Flame (2004) in press.

•

Med Colket, United Technologies Research Center, USA. Most sectional/moment methods for calculation of soot growth in flames utilize a constant particle density of 1.8 gm/cc. A few modeling methods consider a precarbonization, lower density value of about 1.2 gm/cc. Particle density, of course, is a key parameter for estimating particle diameter ($d \sim \rho^{-1/3}$) that in turn is used to compute collision frequencies. The complex, high molecular weight structures shown in your presentation may have effective densities significantly different (lower?) than the normally assumed values; and hence collision frequencies may be incorrectly/inconsistently computed. Do you perceive this as an issue? What are the effective densities of the structures computed in your work?

Reply. The effective densities calculated for the particles at inception are low, ca. 0.4 gm/cc. The collision frequency and sticking probability will also be a function of the molecular configuration. Now that we have configurations for the particles we are calculating the potential surfaces as a function of distance of separation for the purpose of obtaining the effective collision frequency. As shown elsewhere in this symposium [1], the effective sticking coefficient decreases markedly with decreasing size for particles below 10 nm. The particle configuration will be needed to obtain the correct values in this regime.

Reference

[1] A. D'Alessio, A.C. Barone, R. Cua, A. D'Anna, P. Minutolo, *Proc. Combust. Inst.* 30 (2005) 2595–2603. Paper 4A01.

•

Christopher J. Pope, USA. The work presented describes the effects of different fuels. I am curious as to which effects, if any, have been observed due to pressure or temperature, especially with respect to the number and placement of five-membered rings, including corannulene-like rings. Could your simulations predict such structures as fullerenes or soot with an "onion" structure under certain conditions?

Reply. We show in the paper different structural effects (curvature) depending on the flame fuel. In principle fullerenes and onion structures can be produced. The potential used for the MD module treats to some extent the dispersion interactions that are significant in onion-type compounds. However in this work, the only process considered was the addition of small molecules to an existing seed molecule or particle. Future studies will in-

clude the interaction with larger molecules through Van der Waal forces; these are more likely to lead to onion-like structures than chemical reactions.

●

H. Jander, Institute of Physical Chemistry, Germany. In your model you considered the different reactivities of the PAH. Did you distinguish in your model between σ-PAH-radicals and π-PAH-radicals?

Reply. The various forms of radicals, including σ- and π-PAH radicals yield different rate constants, which are in turn reflected in the input from ab initio calculations and experimental data into the KMC module of the KMC/MD code.